18th International Conference on Structural Mechanics in Reactor Technology (SMiRT 18)
Beijing, China, August 7-12, 2005
SMiRT18-D04-1

HIGH CYCLE THERMAL CRAZING: A PHENOMENA RELATED TO THE STRUCTURE

S. Taheri
EDF-R&D-AMA, UMR-EDF-CNRS 2832
1 avenue du Général de Gaulle 92141
Clamart cedex, France
Phone: +33 1 47 65 32 60
Fax: +33 1 47 65 41 18
E-mail: said.taheri@edf.fr

E. Galenne
EDF-R&D-AMA, UMR-EDF-CNRS 2832
1 avenue du Général de Gaulle 92141
Clamart cedex, France

ABSTRACT

The aim of this paper is to give an explanation of crazing observed in some areas of residual heat removal systems (RHR) in French PWR plants. High cycle thermal crazing is explained through the arrest of cracks initiated at surface, in the thickness of the component due to high stress gradient related to high frequencies of thermal load. The conclusion is that there is no difference between high cycle thermal and mechanical fatigue in term of metal behaviour. A parametric study is realised which gives in the case of a thermal periodic loading some bounds for load frequency in function of crack arrest depth. On some RHR the crack network configuration is explained through the sign of weld residual stress in relation with strain control. Far from the weld the presence of crack network under high compressive stress for stainless steels is explained by detrimental effect of pre-hardening on fatigue life in strain control in opposition with stress control. We conclude that shot peening may be detrimental in thermal fatigue.

Keywords : thermal fatigue, crazing, shot peening, pre-hardening, weld residual stress, stainless steel, RHR

1. INTRODUCTION

High cycle thermal fatigue is a generic problem of the residual heat removal system (RHR) in French PWR plants made of 304L stainless steel. It is observed through the presence of a dense, shallow, uniaxial or multiaxial crack network. The work carried on has two aims:

- Understand the existence of thermal crazing in high cycle thermal fatigue where there is no such phenomena on PWR component under mechanical loading. This phenomena is explained by the arrest of cracks in the thickness due to high stress gradient related to high frequencies of thermal loading **[**Taheri 2004-a**]**. From this result we deduce that the difference between high cycle thermal and mechanical fatigue is only related to the structure and not to the behaviour of the metal. Purely mechanical analysis may so be admitted in the case of high cycle thermal fatigue.

- Understand why in some area of RHR there is thermal crazing and in some other there is not, where the loading seems to be the same in both areas. Comparing the crack network configuration with simulations we show that near the weld the configuration of crack network is related to the sign of residual stress. In fact there is absence of crack network under elastic compressive residual stress while cracks are observed under tension residual stress **[**Taheri 2004-b**]**. More over the presence of crack network in areas under high compressive stress is explained by detrimental effect of pre-hardening in strain control (high cycle thermal fatigue) in opposition with stress control. As the pre-hardening is related to surface finishing, we deduce that shot peening may be detrimental in high cycle thermal fatigue.

2. EXPLICATION OF THERMAL CRAZING THROUGH STRUCTURE EFFECT

The main goal is to understand the existence of a dense shallow and multidirectional crack network in high cycle thermal fatigue and its absence in high cycle mechanical fatigue in PWR plant components.

2.1 The reason of high density of crack network in thermal crazing

In mechanical HCF for a usual homogeneous tension compression fatigue test the initiation is the essential part of the life. When a crack is initiated on a privileged site (for example stress concentration due to surface finishing) the rupture is rapidly produced. In the case of a structure for example a pure bending of a rod once a crack initiated the SIF (stress intensity factor) is an increasing function of crack length: there is no possibility for arrest of a crack. There is not enough time for other cracks to initiate because of the large dispersion band of fatigue limit in HCF and consequently there is a very small probability to detect a dense crack network.

In mechanical LCF, because of the plasticity there are less privileged sites for initiation, as plasticity destroys the stress concentration sites on the surface. Moreover the initiation time is a small part of the lifetime. When one crack is initiated there is enough time for another to initiate before the rupture (narrow dispersion band of fatigue limit in LCF). So a dense crack network may exist, but these cracks are usually in plans making an angle of about 45° with principal stress axes.

Tests on homogeneous samples show that there is no difference in fatigue behaviour of a 304L stainless steel in mechanical and thermomechanical fatigue for a number of cycles between 10000 and 100000 [Haddar 2003]. It is difficult to do tests with higher number of cycles for a homogeneous case due to the time needed for tests. For a AISI304 stainless steel upon 10^5 cycles most of the lifetime is in initiation [Socie & Marquis 2000]. For a 2D structure submitted to thermal fatigue, the following analysis may be proposed. An infinite band of finite thickness is submitted on one side to a cyclic thermal sinus loading (Figure 1). For some frequencies of loading, the SIF amplitude may fall down under the limit of non-propagation ΔK_{th} and so the crack stops propagating. Therefore it is possible for a second crack to initiate -because of dispersion band on fatigue limit- out of the shielding effect of the first crack. As the second crack may also stop, this permits another crack to initiate and so on. A crack network is then created ; the distance between cracks is controlled by the shielding effect. The arrest (or the very slow propagation) of cracks in the thickness at 2 mm depth is confirmed by observation on an important number of RHR [Molinie & al, 2002].

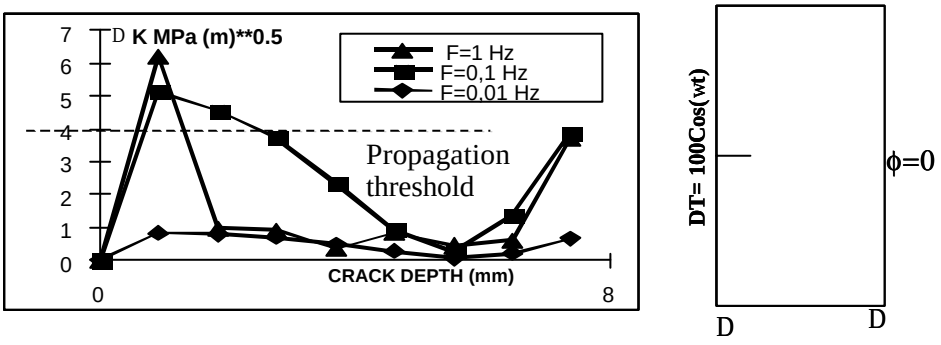

Figure 1 - SIF amplitude versus frequency of thermal loading

The morphology of crazing in 3D thermal fatigue may be deduced from the previous arguments. The Figure 2 shows a pure bending of a parallelepipedic structure with a semi-elliptical crack. Normalized values of K_I at points A and C -the extremity of semi-elliptical crack in the depth and on the surface- are depicted [Rajou & al 1989]. Simulations are realized for the values of a/t equal to 0.2 where t represent the thickness of the plate. The presence of a dense crack network on the surface may be explained in the following way : for $K_I(A) > K_I(C)$ (resp. $K_I(A) < K_I(C)$) the rate of crack propagation is higher on A (resp. C). In presence of a threshold K_{th} (ΔK_{th} in fatigue) the equilibrium value of eccentricity a/c, where a is the crack depth is defined by $K_I(A) = K_I(C) = K_{th}$.

It may be concluded that if the crack stops to propagate at point A, the propagation at point C will also be stopped more or less quickly. This is an explanation of high density of cracks on the surface. For the case of pure bending the equilibrium position is represented by the eccentricity a/c=0.6. For the case of pure tension the equilibrium position is nearly a half circle. It may be so supposed that for large spatial gradients issued from thermal loading semi-elliptical cracks are more elongated (see paragraph 2.3).

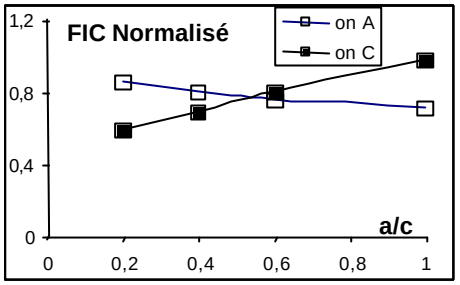

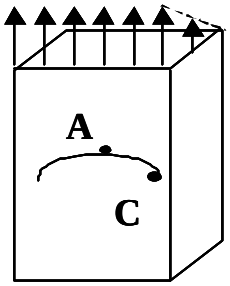

Figure 2 - Normalized SIF on versus eccentricity of semi-elliptical crack a/c for pure bending

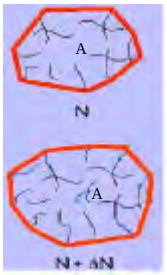

Figure 3 - Densification of crack network after arrest of some cracks

The analysis presented here is justified by tests on a structure device [Maillot & al 2005]. The specimen geometry is parallelepipedic. It is continuously heated by joule effect at a high temperature and it is cyclically submitted to thermal shocks by water spray on the two opposite sides. Figure 3 [Maillot & al 2005] shows schematically the crack network at N and N+ΔN cycles. It is noticeable that during the ΔN cycles existing cracks have not propagated at area A whereas new cracks appear in this area. As it may be supposed that the loading is identical in the area, it may be confirmed that the arrest of crack permits a densification of crack network.

2.2 Multi-directionality of the crack network

For a long tube submitted to a difference of temperature between internal and external skins the values of axial and circumferential stresses are identical. However, in industrial situation stresses –and so crack initiation in high cycle fatigue- may not be the same in the two directions because of different mean stresses or structural effect. So the biaxiality of crack network may not be explained by the simultaneity of initiation: cracks may be created preferentially in the direction where fatigue damage is more important. But as these cracks may stop as explained before, cracks in an orthogonal direction may appear.

Therefore unidirectional or multidirectional cracks may be obtained under thermal loading, and an unidirectional network may become multidirectional under thermal loading if there is no rupture.

2.3 Some parametric studies for the crack arrest under axisymetrical thermal loading : a possible methodology for determination of loading characteristics

Figure 4 shows an aspect of crazing on a RHR. Data analysis on thermal fatigue over all French Power RHR shows a maximum crack depth of about 2 mm for 900 MWe plants (thickness of RHR of about 12 mm) and 2.5mm for 1300 and 1450 MWe plants (thickness of RHR of about 10 mm) [Molinie & al, 2002]. These experimental crack depths will be justified through some parametric studies.

A 2D complete parametric study has been realized through analytical formulation [Musi 2001]. However this analysis does not take into account the fatigue threshold neither the notion of short crack. Here the parametric study takes into account both of them. Results are obtained by FE simulations. The parametric study has been realized on a long tube submitted to a sinus thermal loading on the internal surface. In such a situation the values of axial and circumferential stresses are identical.

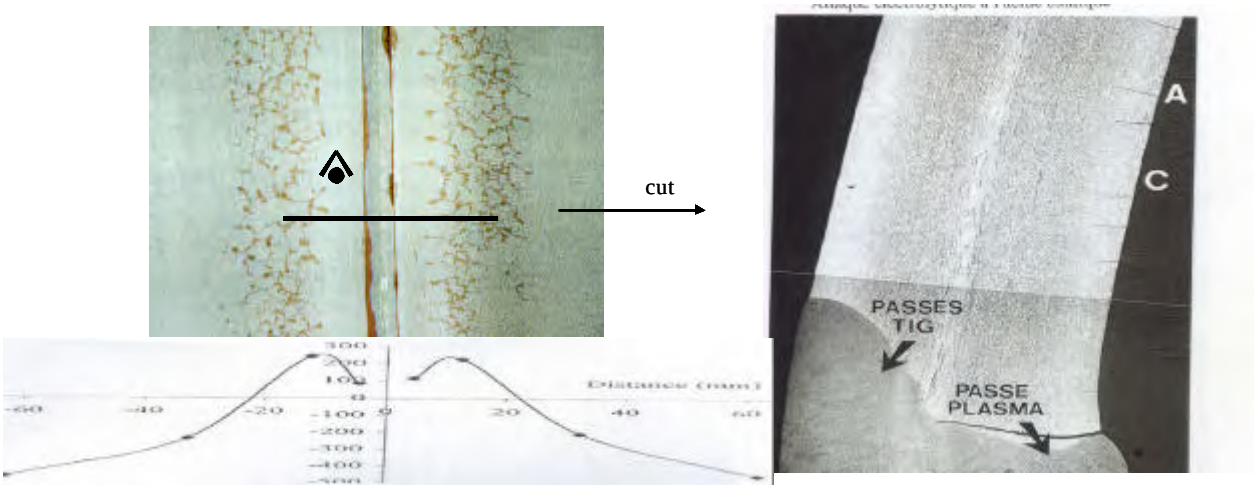

Figure 4 - Thermal crazing on surface related to weld residual stress and crack aspects in the thickness

Geometrical characteristics: The height of the tube is 200 mm. The mean radius is about 112 mm. Different values of thickness (e) will be used to represent different RHR in French PWR plants.

Material data:

-Density * specific heat (J/mm^3/°C, defined at 100°C) : $\rho C_p = 3.85.10^{-3}$

-Thermal conductivity (W/mm/°C, defined at 100°C): $\lambda = 15.86.10^{-3}$

-Heat transfer coefficient (h): different values are used ; the minimal value is 15000 W/m²/°C

-Young Modulus: 198 500 MPa

-Poisson ratio: $\nu = 0.3$

-Thermal expansion coefficient α (defined at 20°C): $1.64.10^{-5}\ K^{-1}$

-Nominal value of threshold for long cracks (2D-Plane): $K_{th} = 170\ MPa\sqrt{mm}$

-Limit size for small cracks (2D-Plane): 0.5 mm

Loading: The thermal loading on internal skin is a heat transfer between the structure and a fluid which temperature varies cyclically between 20 and 180°C (sinus loading). The external skin is supposed to be adiabatic (no heat transfer). Different frequencies of loading and different heat transfer coefficient have been used. Initial state of structure is at 20°C. Mechanical mean stress is supposed to be equal to zero, in this case $K_{\max} = \Delta K / 2$.

Simulations: Non-linear thermal simulations are realised and contact conditions are used on the crack lips. It has been tested that the non-linear simulations may be replaced by a linear one without an important error. Material property are thus taken constant (defined at 100 °C). Simulations are realised with *Code_Aster* (numerical simulation software for structural analysis developed by EDF-R&D).

2D-AXI results: the crack is supposed to be in the middle of the tube. The mesh is given on Figure 5a. Here the effect of different parameters are studied: load frequency, tube thickness and heat transfer coefficient.

Load Frequency: On Figure 5b are compared Kmax (maximum of SIF on a cycle of thermal loading) for different frequencies 5, 3, 1, 0.1 Hz and for a tube thickness of 9.3 mm. The only possible frequency between these 4 frequencies in agreement with an arrest of crack at about 2mm depth is 1 Hz. For 0.1 Hz there is no

arrest of crack because Kmax is an increasing function of crack length. For 5 and 3 Hz the value of Kmax is under the threshold value, so the crack length is less than 0.5 mm which is the limit length for short cracks.

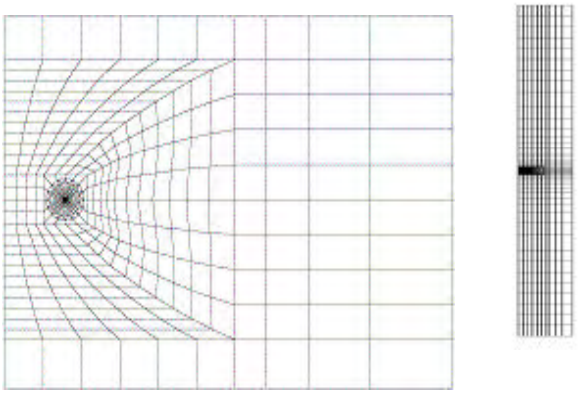

Figure 5a - 2D mesh

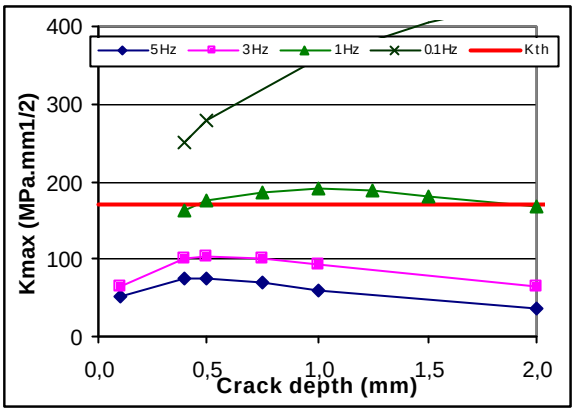

Figure 5b - Evolution of Kmaxversus crack depth for h=15000 W/m²/K, e=9,3 mm, ΔT=160 °C

Thickness of the tube (e): Figure 6a shows a comparison of Kmax for different tube thickness. It shows obviously that the depth of crack arrest is deeper for a thin tube than for a thick tube.

Heat transfer coefficient: On Figures 6b-d, Kmax is depicted for different values of h and different values of frequency. Minimal and maximal values of h are supposed to be respectively 15000 W/m²/K and 50000 W/m²/K. It is noticeable that for 0.1 Hz there is no possibility for crack arrest whatever h, while for 3 Hz all cracks stop before 1.2 mm depth. At 1 Hz the maximum crack length varies from 1.9 to 3.9 mm.

Kmax is also depicted for an infinite value of h (imposed temperature). It may be remarked that the difference in Kmax for h infinite or h=50000 W/m²/K is increasing with the frequency of the loading.

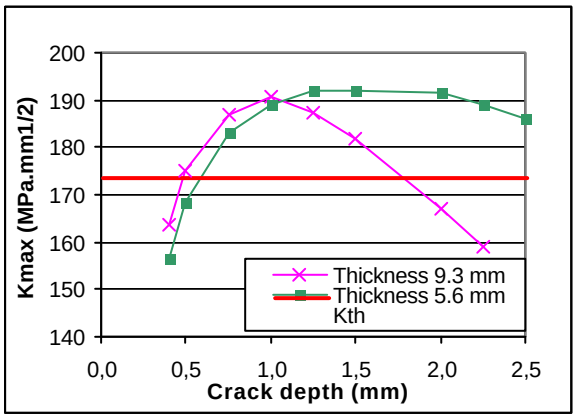

Figure 6a - Evolution of Kmax versus crack depth h =15000 W/m²/K, f=1 Hz, ΔT=160 °C

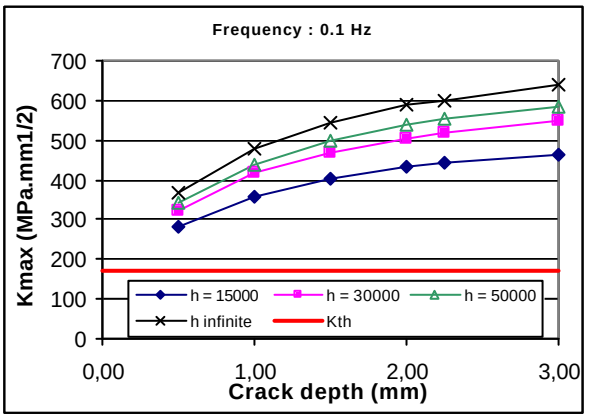

Figure 6b - Evolution of Kmaxversus crack depth for f=0.1 Hz, e=9,3 mm, ΔT=160 °C

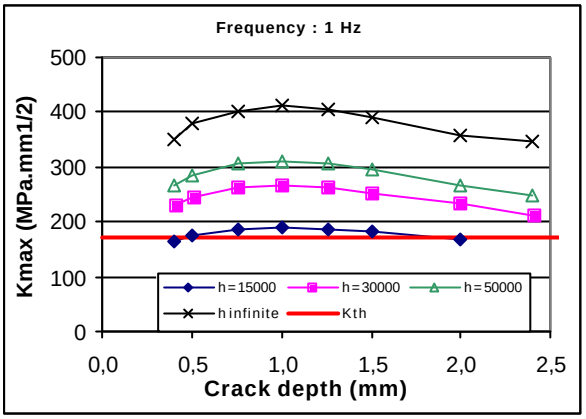

Figure 6c - Evolution of Kmaxversus crack depth for f=1 Hz, e=9,3 mm, ΔT=160 °C

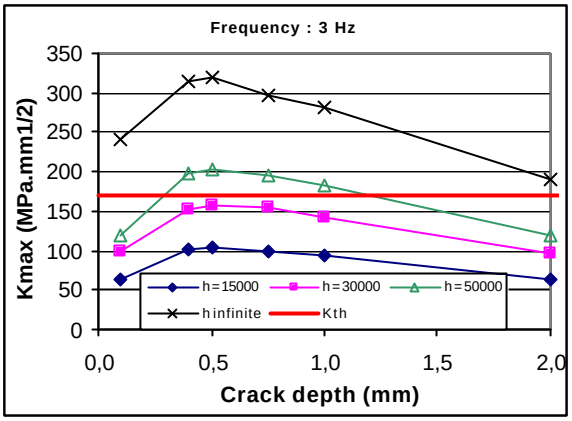

Figure 6d - Evolution of Kmaxversus crack depth for f=3 Hz, e=9,3 mm, ΔT=160 °C

***3D results**:* The semi-elliptical crack is supposed to be in the middle of the tube and orthogonal to the axis of the tube. The propagation is supposed to be governed by 2D Paris law in the plan of the crack and perpendicularly at each point of the crack front.

Comparison 2D-AXI and 3D: classical results are obtained. For the same depth Kmax is larger for a 2D_AXI crack than for an elliptical crack. When a/c decreases the 3D result converges toward 2D_AXI solution (Figure 7). Consequently the use of 2D_Axis simulation represents a penalising approach.

3D crack stabilisation ratio a/c: In paragraph 2.1 an equilibrium value of the eccentricity a/c=0.6 was found for a pure bending test. This eccentricity is lower for a thermal loading with high frequency because the stress gradient decreases with the thickness. Figure 8 shows that for a frequency equal to 1 Hz, for a crack depth a=1 mm and for a/c =0.2, Kmax is nearly a constant value along the crack front. So the semi -elliptical crack is in an equilibrium situation. For a 2 mm-thick crack Kmax is higher at the edge so there would be a more important propagation at the edge: consequently the eccentricity at equilibrium a/c will be smaller than 0.2 for 2mm depth. This is in agreement with some experimental results showing an eccentricity of about 0.05 [Cornuel & Fradet, 2004].

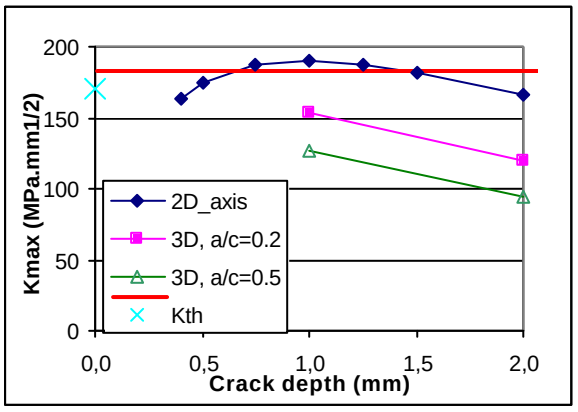

Figure 7 - Evolution of Kmax versus crack depth for 2D and 3D cracks, e=9,3 mm, h =15000 W/m²/K, ΔT=160 °C

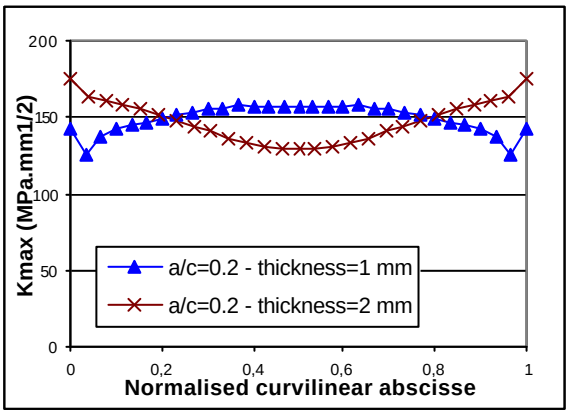

Figure 8 - Kmax versus curvilinear abscissa along the crack front , f=1 Hz, e=9,3 mm, ΔT=160 °C

Conclusions: All results have been gathered in table 1. The conclusion is that for constant amplitude loading, with ΔT =160°C and for any heat transfer coefficient upon the minimum value h=15000 W/m²/K, the SIF at 0.1 Hz is always an increasing function of crack length. There is so no possibility of arrest at 2 mm of

thickness. For 5 Hz loading there is no possibility for cracks to have a length upon 0.5 mm (short crack length limitation). For h=50000 W/m²/K, the only frequency giving a depth of about 2.5 mm need a frequency between 1 and 3 Hz. For h=30000 W/m²/K this frequency is around 1 Hz.

2D-AXI	Heat Transfer Coefficient (W/m²/K)	Maximum Crack length
0.1 Hz	15000	> thickness
	30000	> thickness
	50000	> thickness
1 Hz	15000	1.9
	30000	3.3
	50000	3.9
3 Hz	15000	< 0.5
	30000	< 0.5
	50000	1.2
5 Hz	15000	< 0.5
	30000	< 0.5
	50000	< 0.5
3D (a/c = 0.2)		
1 Hz	15000	< 0.5

Table1 - Maximal depth of the crack for different situations (tube thickness: 9.3 mm)

3. POSSIBLE DETRIMENTAL EFFECT OF SHOT-PEENING IN HIGH CYCLE THERMAL FATIGUE FOR STAINLESS STEELS

Shot peening has been used for assessment of fatigue life by the creation of compressive state of stress on the surface of the component. This operation creates also an important hardening. For stainless steels in strain control this hardening reduce the fatigue life under cyclic strain control in opposition with cyclic stress control. This reduction of lifetime may cancel the beneficial effect of compressive stress and make shot peening detrimental in thermal fatigue.

3.1 Effect of pre-hardening in strain and stress control

In design codes it is usually accepted that constraint elastic-plastic situations may be better represented by a strain control approach. It means that HCF on a structure is usually strain controlled, while HCF experimental curves have usually been obtained in stress control because the experimentation is easier. The aim of this paragraph is to show the different effects of pre-hardening on lifetime in strain and stress control.

Fully reversed cyclic tests on solid cylindrical specimens were used to analyse the effect of pre-hardening on lifetime of 304L and 316L stainless steel. It has been shown [Taheri & Doquet, 2003] that a cyclic pre-hardening (10 cycles of +/- 2%) increases the lifetime in stress control tests while it reduces it in strain control tests (figure 9a). In this figure the effect of pre-hardening and mean stress have been separated. In fact even under a mean compressive stress the detrimental effect in strain control may overcome the beneficial effect of a mean compressive stress. More over a monotonic pre-hardening (16%) may also be detrimental to fatigue life in strain control. The explanation comes from the dependence of cyclic strain-stress curve to pre-hardenning for a stainless steel as shown on Figure 9b [Taheri, 1996]. For HCF, the work realized in [Petitjean 2004] shows that surface finishing may be beneficial in stress control tests as far as it has not created a singularity which reduces drastically the initiation part of lifetime.

From these results it may be concluded that shot peening -usually beneficial in mechanical fatigue- may be detrimental in high cycle thermal fatigue for stainless steel. In fact shot peening create a large pre-hardening and a large compressive stress state. In any case a large compressive stress is beneficial for fatigue life. For a stainless steel however in strain control detrimental effect of pre-hardening may cancel the beneficial effect of compressive stress, in contrast with stress control in which the beneficial effect of pre-hardening and compressive stress are added. For a ferritic steel (for example A42) the effect of pre-hardening is negligible on

fatigue life [Taheri & Doquet 2003], so only beneficial effect of compressive mean stress exists. A shot peening is usually beneficial for a ferritic steel.

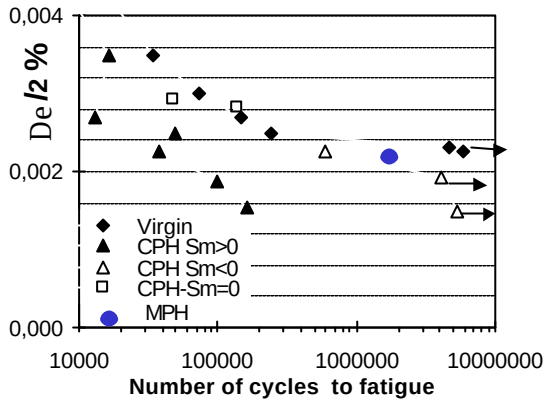

Figure 9a - Effect of cyclic pre-hardening (CPH), Monotonic pre-hardening (MPH) and mean stress Sm on Fatigue life

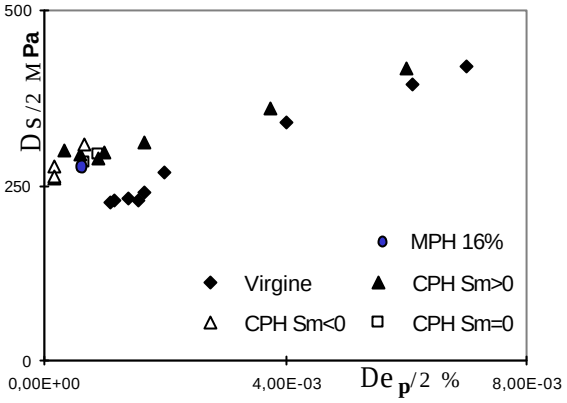

Figure 9b - Effect of cyclic pre-hardening (CPH), Monotonic pre-hardening (MPH) and mean stress Sm on cyclic strain-stress curve

3.2. Simulation of pré-hardening effect with a polycristallin modeling

Simulations using the ENSMP polycristallin modeling [Vogel & al] have been carried on to confirm qualitatively these results. Figures 10a and 10b show simulations realized with *Code_Aster* with a polycristallin modeling on a 316L stainless steel. On figure 10a it may be remarked that in stress control the behavior becomes elastic (elastic shakedown) after pre-hardening, so the lifetime increases while this is not the case in strain control.

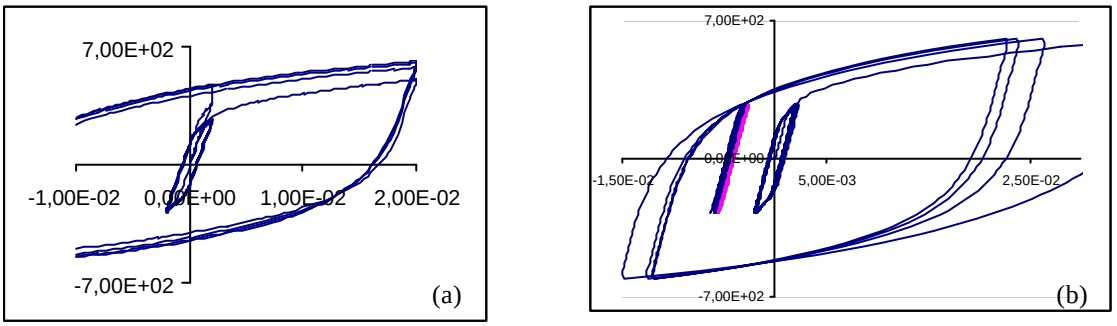

Figure 10 (a, b) – Polycristallin modeling, pre-hardening effect on behavior in strain (a) and stress control (b)

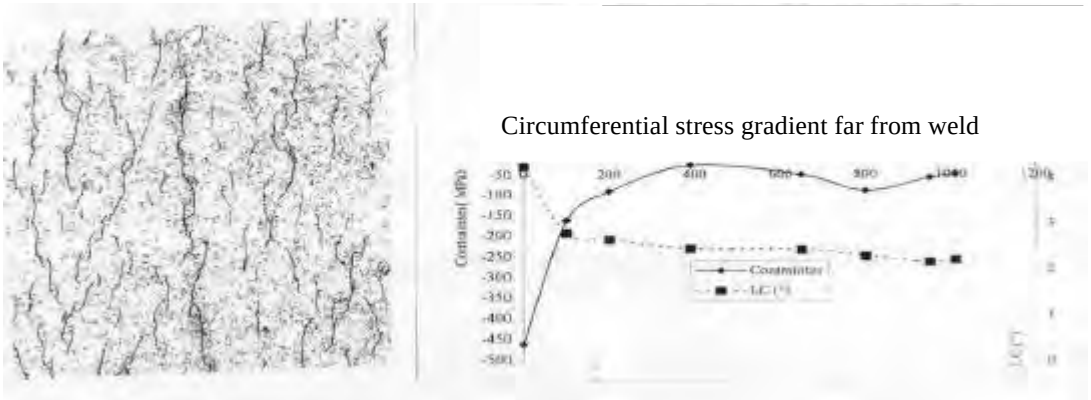

Figure 11 - Crazing in area under high compressive stress

3.3 Application on component

Figure 11 shows a crack network in the area where residual stress is in compression (about -450 MPa). These results may be explained through the analysis presented before: the detrimental effect of pre-hardening in strain control may be able to cancel the beneficial effect of compressive state of stress.

4. WELDING AND DETRIMENTAL EFFECT OF POSITIF MEAN STRESS

Figure 4 shows for a RHR a crack network initiated at the maximum value of the measured axial residual stress. A positive stress on a distance of about the thickness of the elbow (9.23 mm) is found. Figure 12b [Cornuel & Fradet 2004] shows the configuration of crack network in another RHR. We remark parallel axial cracks near the weld, absence of crack after the vicinity of the weld, and presence of crack network far from the weld. The aim here is to show the relation between residual simulated weld stress and the crack network configuration.

In order to validate welding numerical simulation, an experimental mock-up has been designed [Razakanaivo & al 2000]. It consists in an austenitic 316L cylinder with a groove which is full-filled, using TIG process, with thirteen passes of welding. This experimental device is quite representative of an industrial welding process in nuclear field. The experimental program includes an important number of measurements which allows to get several experimental data associated to the process and which are useful to validate numerical simulation. These data are thermal transient, displacement, strain and residual stress measurements. 2D-axisymmetrical numerical simulations of the process are carried on. The results of several modeling are compared with experimental data. As it has not been possible to do any measurement of residual stresses on internal skin the comparison between measure and simulation has been realized on external skin. Quite a good agreement in term of residual stress is obtained between the numerical and the experimental results after 13th pass. On figure 13a [Desroche 2000] the axial and circumferential stresses on internal skin simulated with *Code_Aster* is depicted for the last pass.

These residual stresses on figure 13a may be decomposed into a local effect and a shell effect [Taheri 1989]:

- A pick, tension stress in the vicinity of the weld along a distance of about the thickness h of the structure from the weld tip (this is a 3D effect) ;
- A compression on internal skin (tension on external skin) for which the maximum is situated at a distance of about $\sqrt{h * r_m}$ (where r_m is the mean radius) from the weld (this the global shell effect).

Comparison of the Figures 12a and 12b shows obviously a beneficial effect of quasi elastic residual compressive stress. It may thus be deduced a detrimental effect of positive mean stress. In the vicinity of weld the presence of more cracks perpendicular to the weld is in agreement with the higher value of circumferential weld residual stress. These results are however in contradiction with some experimental results which show a beneficial effect of positive mean stress on test carried on stress imposed for a 304L stainless steel [Petitjean 2004]. In fact the beneficial effect of positive mean stress in some cases may be explained in the following manner: for the same amplitude of stress loading when the mean stress increases the maximal stress increases, this means more pre-hardening and a beneficial effect on initiation for stainless steels which may cancel the detrimental effect of mean stress on initiation and propagation and so give a better life as shown here.

Far from the weld the initiation may be related to detrimental effect of pre-hardening due to surface finishing as explained in section 3.

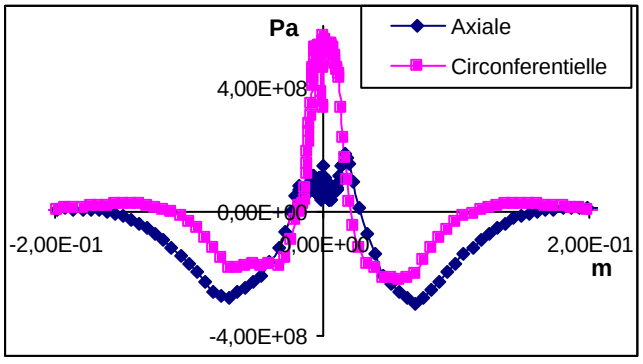

Figure 12a – Residual axial and circumferential weld stress on internal skin

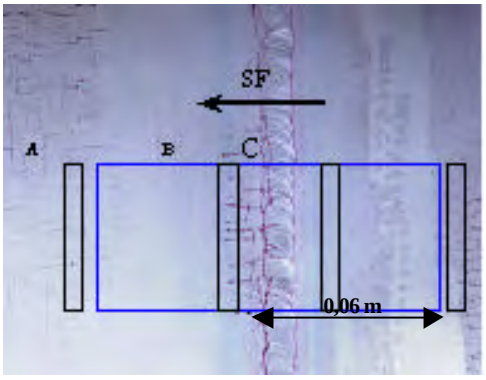

Figure 12b - Configuration of crack network near a weld

CONCLUSION

The existence of high cycle thermal crazing in some areas of residual heat removal systems (RHR) in French PWR plants is explained through the arrest of cracks initiated at surface, in the thickness of the component due to high stress gradient related to high frequencies of thermal load. The difference between high cycle mechanical and thermal fatigue is related only to the structure and not to material behaviour. A parametric study is realised under a periodic loading which gives some indications about the thermal load frequency in function of crack arrest depth. It is shown that to have a crack arrest at about a depth of 2mm for a tube thickness of about 10 mm the thermal load frequency need to be nearly under 3 Hz in a 2D axisymmetrical simulation. Importance of shielding effect on the crack arrest depth has to be considered later.

On some RHR the crack network configuration is explained through the sign of weld residual stress in relation with strain control. Far from the weld the presence of crack network under high compressive stress for stainless steels is explained by detrimental effect of pre-hardening on fatigue life in strain control in opposition with stress control. We conclude that shot peening may be detrimental in thermal fatigue. The semi-qualitative approach presented here has to be extended to a quantitative approach for a determination of the effect of surface finishing and weld residual stress on fatigue life.

REFERENCES

Cornuel F., Fradet F., 2004, rapport EDF/DPN D5710/IECH/2002/008081/1.

Desroche X., 2000, "Simulation numérique d'un essai de soudage sur tube en 13 passe," Internal report, EDF/R&D, HI-75/00/016/.

Haddar N., 2003, PHd Thesis, Ecole des Mines de Paris 2003.

Herbez, E., and O. Goltrant, 1998, "CNPE de Civaux, Tranche 1," Internal report, EDF/GDL, D5710/ECH/1998/009885/01.

Maillot V., Fissolo A., Degalaix G., Degalaix S., 2005, Thermal fatigue crack networks parameters stability : and experimental study. Int. J. of Solids and Structures Vol. 42, N°2, p. 759.

Molinie E., Monteil N., Delatouche S., Roux S., Robert N., Pagès C., 2002, Caractérisation des tronçons RRA 900-1300 MWe deposés. Proceeding of Int. Syposium, Frontevraud.

Musi S. 2002, Note EDF/SEPTEN E-N-ES-MS/02-01018-A : Fatigue thermique des zones de mélange – Description de la méthodologie dite "conventionnelle" d'identification des zones potentiellement sensibles – Développements analytiques associés.

Petitjean S., 2003, "Influence de l'état de surface sur le comportement en fatigue à grand nombre de cycles de l'acier inoxydable austenitique 304L," PhD, université de Poitiers.

Razakanaivo A., et al, 2000, "Tubular welding numerical simulation experimental validation". IERS6, Oxford, UK.

Rajou I.S, Atluri S.N, Newman Jr. J.C, 1989, Stress intensity factors for small surface and corner cracks in plates. Fracture mechanics perspectives & directions ASME 1020.

Socie D., Marquis G.B, 2000, Multiaxial fatigue, Ed. By SAE International.

Taheri S., 1989, "Three dimensional Local Effect and Shell Theories" Int. J. Pres. Ves. & Piping, N° 36, pp. 225-246.

Taheri S., 1996, Multiaxial and fatigue design, ESIS 21 (edited by A. Pineau, G. Cailletaud, and T. C. Lindley), Mechanical Engineering Publications, London, pp. 283-299.

Taheri S., and Doquet V., 2001 Evaluation of non-conservatism of combined Rain flow counting and Miner's rule for damage accumulation in strain controlled fatigue. Washington DC , SMIRT16.

Taheri S., 2004-a, An attempt to analyse crack initiation under high cycle thermal fatigue on a mixing zone of auxiliary cooling System, proceeding of 7th fatigue congress, Berlin, p. 549.

Taheri S. 2004-b, High cycle thermal fatigue on a mixing zone of auxiliary cooling system, proceeding of ASME-PVP conference, San Diego.

Vogel C., Lorentz E., Pilvin P., and Taheri, S. 1997 A constitutive law using a ratchetting stress for description of progressive deformation and comparison with a polycristalline model, Lyon, SMIRT14.

